

# A modified social force model for crowd evacuation considering collision predicting behaviors

Ning Ding<sup>a,\*</sup>, Yu Zhu<sup>b</sup>, Xinyan Liu<sup>a</sup>, Dapeng Dong<sup>a</sup>, Yang Wang<sup>a</sup>

<sup>a</sup> Public Security Behavioral Science Lab, People's Public Security University of China, Beijing, China

<sup>b</sup> Institute of Public Safety Research/Department of Engineering Physics, Tsinghua University, Beijing, China



## ARTICLE INFO

### Keywords:

Pedestrian flow  
Social force model  
Crowd simulation  
Collision predicting

## ABSTRACT

The social force model is one of the most common models used in the study of pedestrian dynamics. In the social force model, there are oscillations in the movement of pedestrians. To address the oscillation phenomenon, this paper modifies the way of setting psychological forces and judgment conditions based on previous research. By comparing the simulation results with the real experimental results, the evacuation time results are basically the same, which validates the effectiveness of the modified social force model. The simulation results show that the modified social force model eliminates the phenomenon of evacuee velocity oscillations near fixed obstacles in the original model and fixes the phenomenon of abnormal behavior of evacuees during collisions. In addition, we simulate different numbers of evacuees (i.e., 25, 50, 100, 200) and the results show that the modified social force model successfully replicates the phenomenon of arch congestion during evacuation.

## 1. Introduction

Many aspects of human social behavior can be simulated using physical methods. [1] Due to the high cost, long duration, site constraints, and unnecessary risks imposed by real-human evacuation experiments, coupled with the rapid development of computer technology, simulation modeling of crowd evacuation behavior using physical methods has become an important method for studying pedestrian evacuation. [2] When the evacuation model was first developed over the course of the last century, researchers studied crowds and introduced a number of techniques to analyze pedestrian flow from a macro perspective, including the hydrodynamics model [3], aerodynamics model [4], and Maxwell Boltzmann distribution [5]. However, compared to a microsimulation model, this type of model has lower precision. It is unable to define the specific behavioral traits of each person, and so can only model the general process of the crowd's evacuation. During the WTC 911 incident, many people died due to untimely evacuation [6]. The tragic repercussions of this incident have garnered worldwide scrutiny, leading to a transformative phase in evacuation research. In this new stage, researchers and building safety designers shifted their focus to pedestrian persons, as opposed to the collective pedestrian flow.

As evacuation simulation models have evolved, social force models, cellular automata models, and agent-based models have come to the forefront. The Social Force Model (SFM) is applied by many commercial evacuation simulation software packages, such as Pathfinder and AnyLogic. The concept of social force was first proposed in 1995 [7]. Several kinds of social forces include (a) the self-driving force that describes the direction of accelerated motion, (b) the repulsive force reflecting the circumstance where

\* Corresponding author.

E-mail address: [dingning@ppsc.edu.cn](mailto:dingning@ppsc.edu.cn) (N. Ding).

pedestrians maintain a certain distance from others and obstacles, and (c) the physical force caused by the contact of evacuees with other people or obstacles. These social forces represent the internal motivation of a pedestrian's behavior and determine the dynamics of crowd movement. They can describe pedestrians' self-psychology, the interpersonal interactions among pedestrians, and the physical interactions between pedestrians and their surroundings. Pedestrians can be conceptualized as particles possessing specific mass and size, which allows us to anticipate their movement in defined directions at specific speeds. The social force model is a continuous micro-model driven by multiple particles. The Cellular Automata (CA) model, another popular micro-model, is noteworthy for its straightforward principles and high efficiency [8,9]. It was originally used to simulate the self-replication phenomenon that characterizes life [10].

The social force model has now been effectively used to examine pedestrian dynamics, such as emergency evacuation and pedestrian flow. It can also reproduce the typical phenomena in crowd evacuation, including group behavior [11], competition [12], and cooperation [13], etc. However, the original model features some unresolved problems, such as the inability to evacuate through narrow exits caused by excessive psychological force at the exit corner, and the model has the Table-Tennis Phenomenon. It refers to the fact that in the original social force model (Helbing's social force model) simulated pedestrians in the model do not accurately reflect actual pedestrian movements, showing oscillatory behaviors and repulsive behaviors that are inconsistent with reality. Therefore, a more accurate model is urgently required to solve existing problems in crowd evacuation.

To solve the issues mentioned above, this paper further improves upon the research achievements of the previous model by improving the psychological force. The second section summarizes the research on the evacuation simulation model and improved social force model. The third section introduces the research foundation of this paper, which focuses on the improvement of the psychological force in the social force model. Then, the valuing and judging conditions of the psychological force are further improved, and a new social force model is constructed. The fourth section encompasses the conducted simulation experiments involving pedestrians evacuating in different scenarios.

## 2. Literature review

### 2.1. Evacuation simulation model

The study of crowd evacuation simulation models is currently at a very advanced stage. It can be broadly divided into two categories: discrete models and continuous models. The representative of the continuous model is the social force model [4], which regards the pedestrian as a particle with a certain shape. It describes the stress that pedestrian has suffered through self-driven force, as well as the contact and non-contact repulsion given by other pedestrians and the environment. Then it solves the motion equation to obtain the new spatial position of the pedestrian and iterate it. The social force model may simulate how people evacuate in public areas. Wan et al. [14] proposed a method for simulating crowd evacuation in the event of bioterrorism in a subway station environment combining the Social Force Model and the Gaussian Puff Model. The model can also be used to show how other types of pedestrian behaviors, like competition, clustering, and herding, might occur during an evacuation. Liu [15] explored the relationship between terrorist attack behavior and pedestrian avoidance behavior from a complex systems perspective by developing a social force model to study crowd evacuation in the event of a terrorist attack in a public place. Zhou et al. [16] used a social force model to study the evacuation time of luggage-laden pedestrians, ordinary pedestrians, and panicked pedestrians in subway stations. Simultaneously, the Social Force Model is adopted and implemented in the bottleneck passage. This analysis reveals that the count of pedestrians carrying luggage is a manageable factor contributing to prolonged evacuation times at bottlenecks. Researchers have conducted various research and gained developments in the spheres of setting social force [17,18], moving direction [15], parameter selection [14], as well as influencing factors [19,20]. They have also applied the model widely to many scenes, such as fire disasters [21], bottleneck areas [22], the room in smoke with multi exits [23], staircases [24], etc. Furthermore, the social force model finds utility not solely in evacuation simulations but also in pedestrian flow simulations, as exemplified by its application in Massmotion, Simwalk, and Viswalk.

Wang et al. [25] simulated pedestrian characteristics, crowd behavior, and the environment through the social force model, and completed the evacuation simulation experiment in the building. Benseghir et al. [26] combined the social dynamics model with fire dynamics to study the evacuation process when the fire is spreading. Kang et al. [27] used the social force model to conduct the evacuation experiment in a shipwreck accident. They incorporated pedestrians' psychological tendency to slide down the slope into their evacuation behavior modeling of the ship's inclined deck. Han et al. [28] used the social force model to simulate pedestrians' emergency evacuation in public places. The model includes the collision-avoidance strategy and the information transmission model that considers information loss. The experiment optimized the emergency evacuation scheme in large public areas. They established a joint social force model appropriate to the actual condition of sudden toxic gas events. Some scholars have also studied avoidance-based collision prediction models. Zanlungo et al. [29] improved the social force model using a genetic algorithm to label pedestrian trajectories and were able to accurately predict when and where the next collision would occur. Cambuim et al. [30] proposed an FPGA-based implementation of the pedestrian detection (PD) system based on HOG and SVM techniques, supporting image pyramids and detection windows of different dimensions. Rinke et al. [31] developed a multi-layer approach for representing the movement of road users and their interaction, based on the social force model. It allows qualitative testing of circumvention strategies and computes realistic results with good performance. El-Basyouny et al. [32] advocated the use of multivariate Poisson-lognormal (MVPLN) regression to develop models for collision count data., and presented an alternative approach for quantifying the effect of the multivariate structure on the precision of expected collision frequency.

Cellular Automata (CA) stands as one of the exemplary discrete models. Firstly, the space is discretized. Each person occupies a cell, and then rules are applied to judge the position movement of personnel in each iterative time step. Initially, it was Blue [33], Klüpfel

[34] and others who introduced the cellular automata model into the field of crowd evacuation simulation. However, due to its simplexes of calculation and wide range of applications, it has received long-time development. Researchers have greatly promoted the application of cellular automata [35]. In the field of pedestrian evacuation by modifying interaction rules [36], changing the shape of cells [37], adding influencing factors [38], etc. Lattice gas model can be regarded as a variant of cellular automata model. The difference lies in that pedestrians no longer occupy the cells of the grid, but occupy the lattice points of the grid. It is also widely used in the field of pedestrian evacuation simulation [39,40]. Apart from these two categories, some researchers have also proposed some special evacuation models, such as the velocity-based model [41,42], bio-crowd model [43], magnetic force model [44,45], centrifugal force model [46], snowdrift game model [47], generalised centrifugal force model [48], etc.

## 2.2. Improved social force model

The social force model was first proposed in 1995. [7] The acceleration and speed of pedestrians are based on Newton's second law. These forces emerge through the collective interplay of the self-driven force arising from pedestrians' awareness, the mutual repulsion between pedestrians, the repulsion between pedestrians and boundaries or obstacles, attraction forces originating from interactions between pedestrians or objects, and the random disturbing forces stemming from disruptive behaviors. After that, though it has been improved, it still contains several deficiencies. Based on this improved social force model, other scholars have further enhanced and refined the social force model.

Aiming at the problem of overlapping pedestrians, Seyfried et al. [49] proposed a mechanism to stop pedestrians automatically. Parisi et al. [20] put forward the respect factor and thus accomplish the pedestrian deceleration mechanism. Chen et al. [50] and Gao et al. [51] improved the social force model using relative speed and reduced the problem of pedestrian oscillation. In addition, many researchers have studied and improved the social force model in the aspects of parameter selection [52], anisotropy of pedestrian movement [52,53], pedestrian density [54], demanding space analysis [55], and algorithm optimization [56], etc.

When simulating crowd evacuation, Kaup et al. [57] use the form of attraction and exclusion to express the pedestrians' characteristics such as age at the group level. Zhang et al. [58] improved the social force model and proposed a multi-exit evacuation model based on a continuum model. Among them, the multi-exit selection model of pedestrians considers the distance between pedestrians and exits, the density of pedestrians near exits, and the width of exits. The pedestrian evacuation model considers the impact of pedestrian psychological factors on the expected speed and attraction of exits. Liu et al. [59] proposed a new mechanical model to simulate evacuation processes in complex environments. Compared with the existing models, this model considers more environmental factors from the motivation level and decision-making level. Lei et al. [60] used the improved social force model to study the relationship between the number of tour guides, their locations, the number of exits, and the resulting evacuation time. Liu et al. [15] used the improved social force model to study the evacuation problem in public places during terrorist attacks and found that the distribution of terrorists' starting positions has a great impact on the number of casualties. Liu et al. [61] proposed an improved social force model where pedestrians consider avoiding potential conflicts in advance during the walking process. Simultaneously, the simulation results show that conflict avoidance makes pedestrian trajectories smoother and more realistic. Chenet al. [62] further discussed the perspectives of description ability, parameter calibration, and flexible application in a complex environment. They also proposed a framework in terms of assessment criteria for pedestrian models taking into consideration pedestrian attributes, motion base cases, self-organization phenomena, and some special cases.

## 3. Modified social force model

In the original social force model, there is an unrealistic phenomenon caused by the collision between personnel and fixed obstacles. This paper called it the able-Tennis Phenomenon. To address this unrealistic phenomenon, this paper improves the size of the Time-Headway force and the conditions for generating psychological force, based on Gao's research. [51] Time-Headway force refers to the wish to retain a certain time distance, while Collision-Avoidance force refers to the intention of avoidance when one finds that there will be a collision.

### 3.1. The original social force model and a previous modified model

The new stage of developing mechanical model should begin with Helbing's social force model in 1995 and further developed in 2000, and obtained the social force model framework that is still applicable up to now, as shown in Eq. (1):

$$\frac{dv_i}{dt} = m_i \frac{v_i^0(t)e_i^0(t) - v_i(t)}{\tau_i} + \sum_{j(\neq i)} f_{ij} + \sum_w f_{iw} \quad (1)$$

where,  $m_i$  is the quality of a pedestrian,  $v_i$  represents pedestrian's moving speed vector;  $v_i^0(t)$  represents pedestrian's expected speed;  $e_i^0(t)$  represents the expected moving direction of pedestrian;  $\tau_i$  is characteristic time;  $f_{ij}$  represents the interaction between pedestrian  $i$  and other pedestrians  $j$ , including contact force and non-contact force. In the setting of force and according to different sources of force, the social force model can be divided into self-driven force  $f_D$  interaction force  $f_{ij}$  between pedestrians, and the force  $f_{iw}$  between pedestrians and obstacles.

Currently, when there is a difference between the pedestrian's current speed vector and their expected speed vector in the free state, the pedestrian will urge themselves to change their moving speed. The force that corresponds with this behavior is called the self-

driven force, as shown in Eq. (2)  $\tau_i$  is the characteristic time. There exists a similarity between the force composition among pedestrians and that between pedestrians and obstacles. The three sub-items are the psychological repulsion force that pedestrians want to keep a certain distance from other pedestrians and obstacles, the normal elastic force generated after pedestrians contact and extrude other pedestrians or obstacles, and the tangential friction caused by mutual contact during movement, as shown in Eqs. (3) and (4). The function  $g(x)$  is shown as Eq. (5), which is equaled to  $x$  when  $x > 0$ , and equaled to 0 when  $x \leq 0$ .

$$f_D = m_i \frac{v_i^0(t)e_i^0(t) - v_i(t)}{\tau_i} \quad (2)$$

$$f_{ij} = A_i e^{\frac{r_j - d_{ij}}{B_i}} n_{ij} + kg(r_j - d_{ij})n_{ij} - kg(r_j - d_{ij})\Delta v_{ij}' t_{ij} \quad (3)$$

$$f_{iW} = A_i e^{\frac{r_i - d_{iW}}{B_i}} n_{iW} + kg(r_i - d_{iW})n_i W - kg(r_i - d_i W)(v_i \cdot t_{iW}) t_{iW} \quad (4)$$

$$g(x) = \begin{cases} x, & x > 0 \\ 0, & x \leq 0 \end{cases} \quad (5)$$

Our research group studied the collision-avoidance psychology in the process of pedestrian evacuation, improved the previous social force model, and put forward a modified social force model [63]. This model improves on the limitations of previous social force models by considering pedestrians' competitiveness. The improved social force model can modify pedestrians' collision avoidance. Both time headway and time-to-collision are considered indicators of collision. The modified model is validated by experiments finally. In this study, we refer to it as the GSF (Gao's social force model). In accordance with this, SF is the original social force model (social force model). The model that this study is primarily aiming to improve is referred to as MSF (modified social force model) in the next section. Since in SF, the interaction between pedestrians and the interaction between pedestrians and obstacles are very similar, we will rewrite Eq. (1) here.

We will change the original classification according to the source of force to the classification according to the nature of force, and thus obtain Eq. (6). Wherein,  $F_D$  represents self-driven force,  $F_S$  represents the resultant force of psychological force, and  $F_P$  represents the resultant force of contact force. They are determined by Eqs. (7)–(10) respectively. It should be noted that both psychological force and contact force include two situations: between pedestrians themselves and between pedestrians and obstacles.  $\varepsilon_{ij} = R_i + R_j - d_{ij}$  in the Eq. (9) represents the compression between pedestrian  $i$  and pedestrian  $j$ . Based on the analysis of the existing experiment data set and the evacuation experiment data of Liuqing building in Tsinghua University, GSF takes into account the existence of Time Headway  $T^H$  and the Time to Collision  $T^C$  [51]. The psychological force in Eq. (8) is divided into the Time-Headway force  $F_S^H$  and collision-avoidance force  $F_S^C$ , as expressed in Eqs. (11) and (12). Time-Headway force refers to the wish to retain a certain time distance, while Collision-Avoidance Force refers to the intention of avoidance when one finds that there will be a collision. The time headway is the ratio of the current vacant distance to the current moving speed. When the time distance is found to be less than the threshold, the pedestrian's expected speed will be 0 and the moving speed will be reduced until the time distance is sufficient. When it is found that the  $T^C$  of one's own is less than the threshold,  $F_S^C$  will make the normal collision speed of the expected collision be 0 to avoid injury. In terms of effect,  $F_S^H$  will only reduce the moving speed of pedestrians without changing the moving direction of pedestrians.  $F_S^C$  will make the speed direction of the pedestrian and the pedestrian about to collide parallel to each other.

$$m_i \frac{dv_i}{dt} = F_D + F_S + F_P \quad (6)$$

$$F_D = m_i \frac{v_i^0 - v_i^{(t)}}{\tau} \quad (7)$$

$$F_S = F_S^H + F_S^C \quad (8)$$

$$\varepsilon_{ij} = R_i + R_j - d_{ij} \quad (9)$$

$$F_P = kg(\varepsilon_{ij} n_{ij} + kg(\varepsilon_{ij})(-v_{ij} \cdot t_{ij}) t_{ij}) \quad (10)$$

$$F_S^H = \begin{cases} -m_i \frac{v_i^0}{\tau}, & T^H < \tau \\ 0, & T^H \geq \tau \end{cases} \quad (11)$$

$$F_S^C = \begin{cases} -m_i \frac{v_{ij} \cdot n_{ij}}{\tau} n_{ij}, & T^H < \tau \\ 0, & T^C \geq \tau \end{cases} \quad (12)$$

where

$$T^H = \frac{|d_{ij} \cdot \cos\theta| - \sqrt{(2R)^2 - (d_{ij} \cdot \sin\theta)^2}}{|v_i|} \quad (13)$$

$$T^C = \frac{|d_{ij} \cdot \cos\varphi| - \sqrt{(2R)^2 - (d_{ij} \cdot \sin\varphi)^2}}{|v_{ij}|} \quad (14)$$

The constraint condition difference between time-headway force and collision-avoidance force lies in whether the collision object moves or not. Furthermore, GSF also considers the psychological force under different competitive degrees, and uses  $\alpha \in [0,1]$  to represent the overall competitive degree. At this time, the psychological force will increase the coefficient term  $(1 - \alpha)$ . The higher the overall competitiveness, the lower the inclination to avoid collisions and the need for time headway.

Although the above research has modified the psychological force in the social force model to express how pedestrians' psychological needs in terms of time, space, and collision avoidance affect their evacuation behavior, it still has limitations. It solves the problem existing in the original model that pedestrians cannot evacuate through narrow exits due to the excessive psychological force at the exit corner. It also greatly reduces the abnormal Table-Tennis phenomenon that exists in the original social force model that occurs when pedestrians collide with fixed obstacles. However, the GSF suffers from an issue of excessive setting of the time-headway force, which causes a direct cessation of movement when facing stationary obstacles and a reverse movement when facing imminent collision obstacles. GSF only mitigates the Table-Tennis Phenomenon without eliminating it completely. To address this issue, this paper further improves of the time-headway force and collision-avoidance force.

### 3.2. Modified social force model

#### 3.2.1. Improve the time-headway force

As mentioned above, pedestrians will generate time-headway force  $F_S^H$  and collision-avoidance force  $F_S^C$  during their movement. Figs. 1 and 2 have described the environment in which pedestrian generates time-headway force and collision-avoidance force. In the current improved social force model, when we expect that there will be a collision, the time-headway force will be triggered at the same time. Under the effect of two psychological forces overlapping, some abnormal phenomena will occur due to the excessive time-headway force. The following part will analyze these phenomena. When examining the psychological force, we momentarily disregard scenarios in which pedestrians interact with their surroundings or with other pedestrians—that is, pedestrians when,  $F_P = 0$ .

##### Situation 1. a pedestrian only affected by the time-headway force

When the situation in Fig. 1 occurs and pedestrian  $j$  will not collide with pedestrian  $i$  within the expected time, pedestrian  $i$  will only generate the effect of time-headway force. Its stress condition is shown in Eq. (14). After the characteristic time  $\tau$ , the speed of the pedestrian  $i$  will rapidly reduce to 0. It is equal to this situation: when a pedestrian exists at a close distance, the rear pedestrian will immediately stop waiting until the time-headway increases and meets the pedestrian needs. If the pedestrian  $j$  ahead keeps moving at a slow speed, pedestrian  $i$  will move in a "stop-accelerate-stop" phenomenon. This phenomenon is inconsistent with actual situation.

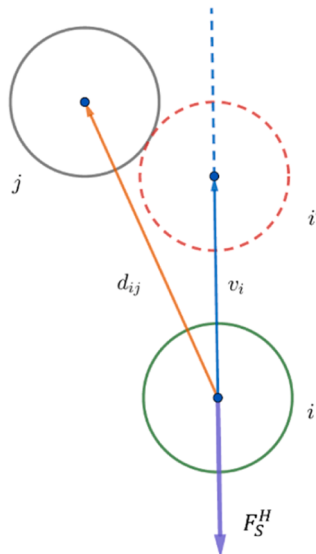


**Fig. 1.** Schematic diagram of time-headway limitation.

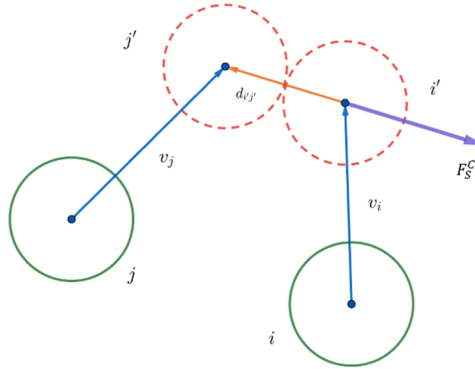


**Fig. 2.** Schematic diagram of expected collision.

$$m_i \frac{dv_i}{dt} = m_i \frac{v_i^0 - v_i}{\tau} - m_i \frac{v_i^0}{\tau} = -m_i \frac{v_i}{\tau} \quad (14)$$

**Situation 2.** a pedestrian affected by the time-headway force and the collision-avoidance force at the same time

When the situation in Fig. 2 occurs, pedestrian  $i$  will foresee that there will be a collision with pedestrian  $j$  within the characteristic time  $\tau$ , which triggers the collision-avoidance force, and necessarily trigger the time-headway force at the same time. The stress condition is shown in Eq. (15). Once the characteristic time  $\tau$  has elapsed, pedestrian  $i$  velocity transforms to  $(v_{ij} \cdot \hat{d}_{ij}) \hat{d}_{ij}$ , with its direction aligned in the opposite direction of  $\hat{d}_{ij}$  as illustrated in Fig. 2. This corresponds to the opposing position of pedestrian  $j$  at the anticipated collision moment. At this time, regardless of the moving speed of pedestrian  $j$ , the moving speed direction of pedestrian  $i$  will become the direction of the connecting line between pedestrian  $i, j$ . It exaggerates the degree of direction change in pedestrians' collision-avoidance behaviors.

$$m_i \frac{dv_i}{dt} = m_i \frac{v_i^0 - v_i}{\tau} - m_i \frac{v_i^0}{\tau} - m_i \frac{v_{ij} \cdot \hat{d}_{ij}}{\tau} \hat{d}_{ij} = -m_i \frac{v_i}{\tau} - m_i \frac{v_{ij} \cdot \hat{d}_{ij}}{\tau} \hat{d}_{ij} \quad (15)$$

According to the generation environment of time-headway force and collision-avoidance force, it can be seen that these two kinds of psychological forces mainly concern with pedestrians or obstacles in front of the moving direction, without considering the influence of obstacles in the side direction. This is one of the key differences between the MSF and GSF.

The problem with the situation described above is that the time-headway force is set too high, causing pedestrians to stop moving when facing stationary obstacles and reverse direction when facing obstacles that are about to collide with them. To solve this problem, this paper further optimizes the time-headway force and collision-avoidance force. The so-called time-headway force comes from the fact that pedestrians want to maintain a certain personal space psychology with the pedestrians in front. On the one hand, pedestrians can obtain a more comfortable walking experience, since aspects including breathing, vision and freedom of movement will all be affected by the size of free space. On the other hand, even if the pedestrians in front suddenly stop moving, the pedestrians in the rear

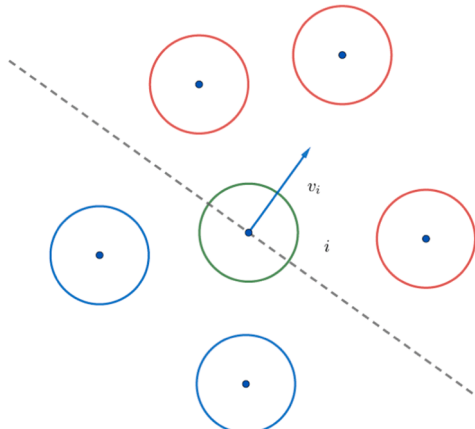


**Fig. 3.** Schematic diagram of the object that generates psychological force.

also have sufficient reaction time. The so-called collision-avoidance force comes from pedestrians' psychology to avoid predictable collisions in the process of moving. In this case, the psychology of avoiding collision will prevail, and the psychological requirements for time headway will reduce. Therefore, this paper sets pedestrians' time-headway force and collision-avoidance force according to the following rules. It will only consider the psychological force generated by the pedestrian and the obstacle in front of the pedestrian, as shown in Fig. 3. Only the red pedestrian may generate psychological force on the green pedestrian  $i$ . Other pedestrians will not be considered temporarily.

It can be seen from above that there are two situations in the calculation of psychological force: The first is that the collision-avoidance force and the time-headway force exist at the same time. The second is that only the time-headway force exists. The model of this passage has modified the time-headway force from Eq. (11). When only the time-headway force exists, the time-headway force is described by Eq. (16). At this time, the time-headway force increases as the time headway of the front pedestrian in Fig. 1 decreases, until it reaches the  $-m_i v_i^0 / \tau$  of the amount before optimization. Its effect is to offset the pedestrian's self-driven force and slow it down.

$$F_S^H = -m_i \frac{v_i^0}{\tau} + m_i \frac{v_i T^H}{\tau^2} \quad (16)$$

When the collision-avoidance force and the time-headway force exist at the same time, it is prior for pedestrian' to avoid collision rather than maintain the time headway space. Therefore, the time-headway force will be taken the smallest in value, that is, make  $T^H = \tau$  in the above equation. Thus, Eq. (17) is obtained. We still use Eq. (12) to describe the magnitude of collision-avoidance force.

$$F_S^H = -m_i \frac{v_i^0}{\tau} + m_i \frac{v_i}{\tau} \quad (17)$$

Under such a setting of time-headway force and collision-avoidance force, we will analyze the two problems mentioned above again. For the case in Fig. 1, when the pedestrian triggers the time headway acceleration, the Eq. (18) about motion state is obtained.

$$m_i \frac{dv_i}{dt} = m_i \frac{v_i^0 - v_i}{\tau} - \left( m_i \frac{v_i^0}{\tau} - m_i \frac{v_i T^H}{\tau} \right) = -m_i \frac{v_i}{\tau} \frac{\tau - T^H}{\tau} \quad (18)$$

At this time, pedestrian  $i$  will decide the speed of deceleration according to the amount of the time headway. A decrease in the time headway leads to a more rapid deceleration. A slower deceleration is the result of a larger time headway. At this time, the pedestrian  $i$  will only slow down but not stop directly when following the low-speed pedestrian  $j$ , which is more in line with the real situation.

For the case in Fig. 2, when the pedestrian triggers the time headway acceleration and collision acceleration at the same time, the Eq. (19) about motion state is obtained.

$$m_i \frac{dv_i}{dt} = F_D + F_S^H + F_S^C = m_i \frac{v_i^0 - v_i}{\tau} - m_i \frac{v_i^0}{\tau} + m_i \frac{v_i}{\tau} - m_i \frac{v_{ij} \cdot \hat{d}_{ij}}{\tau} \hat{d}_{ij} = -m_i \frac{v_{ij} \cdot \hat{d}_{ij}}{\tau} \hat{d}_{ij} \quad (19)$$

At this time, the pedestrian will decelerate along the direction of expected collision. When the expected collision occurs, the speed of the pedestrian has changed to  $v_i - (v_{ij} \cdot \hat{d}_{ij}) \hat{d}_{ij}$  after time  $\tau$ . The speed of the two in the direction of the centerline is 0, which happen to avoid the collision through direction deviation.

### 3.2.2. Improvement towards the generating conditions of the psychological force

The setting of psychological force depicts how pedestrians are feeling as they are moving. It also reflects their decision-making process when they move. When a pedestrian collides with other pedestrians or walls, it will inevitably produce the psychological force that include the time-headway force and collision-avoidance force mentioned above. The judging condition is:

$$|d_{ij}| < 2R \quad (20)$$

When pedestrian  $i$  judges that he will collide with a pedestrian or the wall in time  $\tau$ , it will also produce the time-headway force and the collision-avoidance force. We will analyze judgment conditions at this time below. When analyzing, we will take pedestrian  $i$  as the reference system, then the absolute speed  $v_j$  of the pedestrian  $j$  is transformed into the relative speed  $v_{ji}$  under pedestrian  $i$ 's reference system. At this time, pedestrian  $j$  has three moving states relative to  $i$ , that is, close to  $i$ , far away from  $i$ , and keeping the relative distance unchanged with  $i$ . They correspond to the three states of  $v_{ji} \cdot d_{ji} > 0, < 0$  and  $= 0$ , respectively.

When  $v_{ji} \cdot d_{ji} > 0$ , pedestrian  $j$  is gradually approaching  $i$ . their possible motion state is shown in Figs. 4 and 5. It can be calculated that the conditions for collision are  $|d_{ij}| \cdot \ln \varphi < 2R$ . We record the estimated time that collision occurs as  $T^C$ . When  $T^C$  is greater than the expected collision threshold  $\tau$ , it means that the distance between them is large enough, and there is no need considering the psychological force generated by pedestrian  $j$ . When  $T^C \leq \tau$ , pedestrian  $j$  will collide with  $i$  within the expected time threshold. At this time, the distance between them is small enough so that the time-headway force and collision-avoidance force are produced.

For the case in Fig. 5, we will calculate the expected collision time  $T^C$  as below. In GSF,  $T^C$  refers to the time taken for pedestrian  $i$  to collide with pedestrian  $j$  when he maintains the current moving speed and move forward constantly. At this time, the moving distance is the distance of  $j$  and  $j'$  concentric lines. The calculation result is shown in Eq. (14). In the MSF, we not only considered the current moving speed of pedestrians, but also considers the current acceleration  $\alpha$  of pedestrian  $j$  partially. That is, we mainly consider the

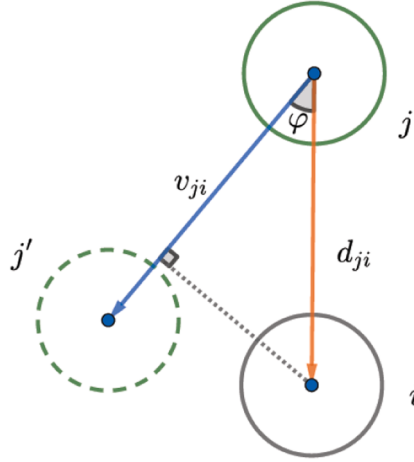


**Fig. 4.** Schematic diagram showing that pedestrians come together without collision.

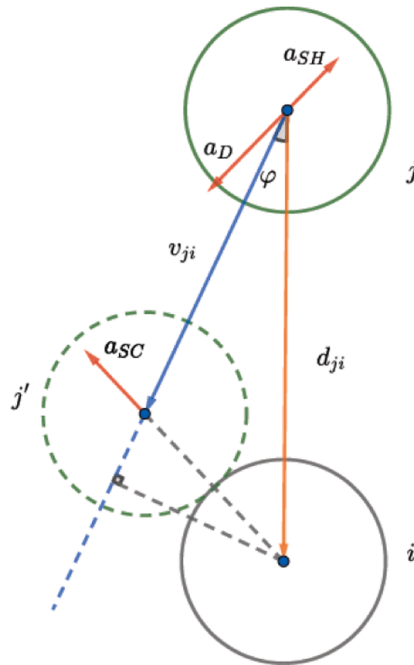


**Fig. 5.** Schematic diagram showing that pedestrians come together and collision happens.

component of pedestrian  $j$  in the direction of  $d_{ij}$ . We can obtain the  $T^C$  satisfactory Eq. (21), and its result is shown in Eq. (22):

$$v_{ij}\cos\varphi \cdot T^C + \frac{1}{2}a_{ji}\cos\varphi \cdot T^{C^2} = \left( d_{ji}\cos\varphi - \sqrt{(2R)^2 - (d_{ij}\sin\varphi)^2} \right) \cos\varphi \quad (21)$$

$$T^C = \frac{-v_{ji} + \sqrt{v_{ji}^2 + 2a_{ji}\left(d_{ij}\cos\varphi - \sqrt{(2R)^2 - (d_{ij}\sin\varphi)^2}\right)}}{a_{ji}} \quad (22)$$

where,

$$\cos\varphi = \frac{d_{ji} \cdot v_{ji}}{|d_{ji}| |v_{ji}|}, \sin\varphi = \frac{d_{ji} \times v_{ji}}{|d_{ji}| |v_{ji}|} \quad (23)$$

When  $v_{ji} \cdot d_{ji} \leq 0$ , pedestrian  $i$  and  $j$  will keep a fixed relative distance or stay away from each other. There will never be collision, so there will be no collision-avoidance force. The psychological state of pedestrians is also relatively relaxed. Therefore, they will consider maintaining the time headway space with other pedestrians as much as possible. When the pedestrian is not affected by psychological force, it will accelerate to the desired speed under the action of self-driven force, and then move at a uniform speed. Here, time headway distance can be understood by making an analogy with vehicle's safety distance. When the front pedestrian  $j$  suddenly stops, pedestrian  $i$  still moves under the action of self-driven force. If it will collide with pedestrian  $j$  within time  $\tau$ , the time headway acceleration will be triggered separately. Fig. 6 shows the motion law at this point. The pedestrian is equivalent to the static state in the analysis. Similar to the analysis in Fig. 5, we need to satisfy  $|d_{ij} \cdot \sin\theta| < 2R$  first to produce time-headway force, and then satisfy the expected collision time  $T^H < \tau$ . The critical condition is that the collision of pedestrians just happens under the action of self-driven force. This process is uniformly accelerated. Therefore, Eq. (24) can be obtained, and the result is shown in Eq. (25).

$$v_i \cos\theta \cdot T^H + \frac{1}{2} a_D \cos\theta \cdot T^{H^2} = \left( d_{ij} \cos\theta - \sqrt{(2R)^2 - (d_{ij} \sin\theta)^2} \right) \cos\theta \quad (24)$$

$$T^H = \frac{-v_i + \sqrt{v_i^2 + 2a_D(d_{ij} \cos\theta) - \sqrt{(2R)^2 - (d_{ij} \sin\theta)^2}}}{a_D} \quad (25)$$

where,

$$\cos\theta = \frac{d_{ji} \cdot v_i}{|d_{ji}| |v_i|}, \sin\theta = \frac{d_{ji} \times v_i}{|d_{ji}| |v_i|} \quad (26)$$

Compared with GSF, MSF has great differences in judging whether psychological force has been produced. GSF only considers the current speed, but not the acceleration. However, MSF considers not only the current velocity, but also the effect of acceleration. In the MSF the judgment of pedestrian psychological force will follow the steps shown in Fig. 7. It should be noted that when the collision-avoidance force exists, the time-headway force has nothing to do with the current time headway. The pedestrian's contact physical force needs to consider all the pedestrians he contacts, while the psychological force only considers the source object with the greatest impact, that is, the psychological force brought by the object with the fastest collision.

#### 4. Simulation

In this paper, MATLAB R2019b is used to realize the modified social force model. The computer operating system is Windows10 64 bit. The main frequency of the host CPU is 1.6 GHz and 1.8 GHz, and the memory is 16GB. In the simulation, the radius of pedestrian is 0.21 m, and the evacuation speed is about 1.34 m per second. The simulation program is calculated every 0.02 s.

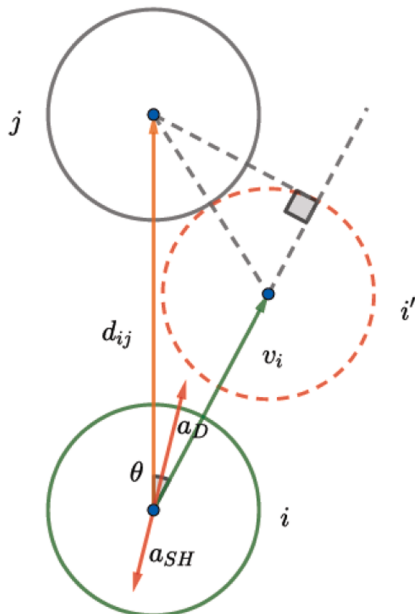
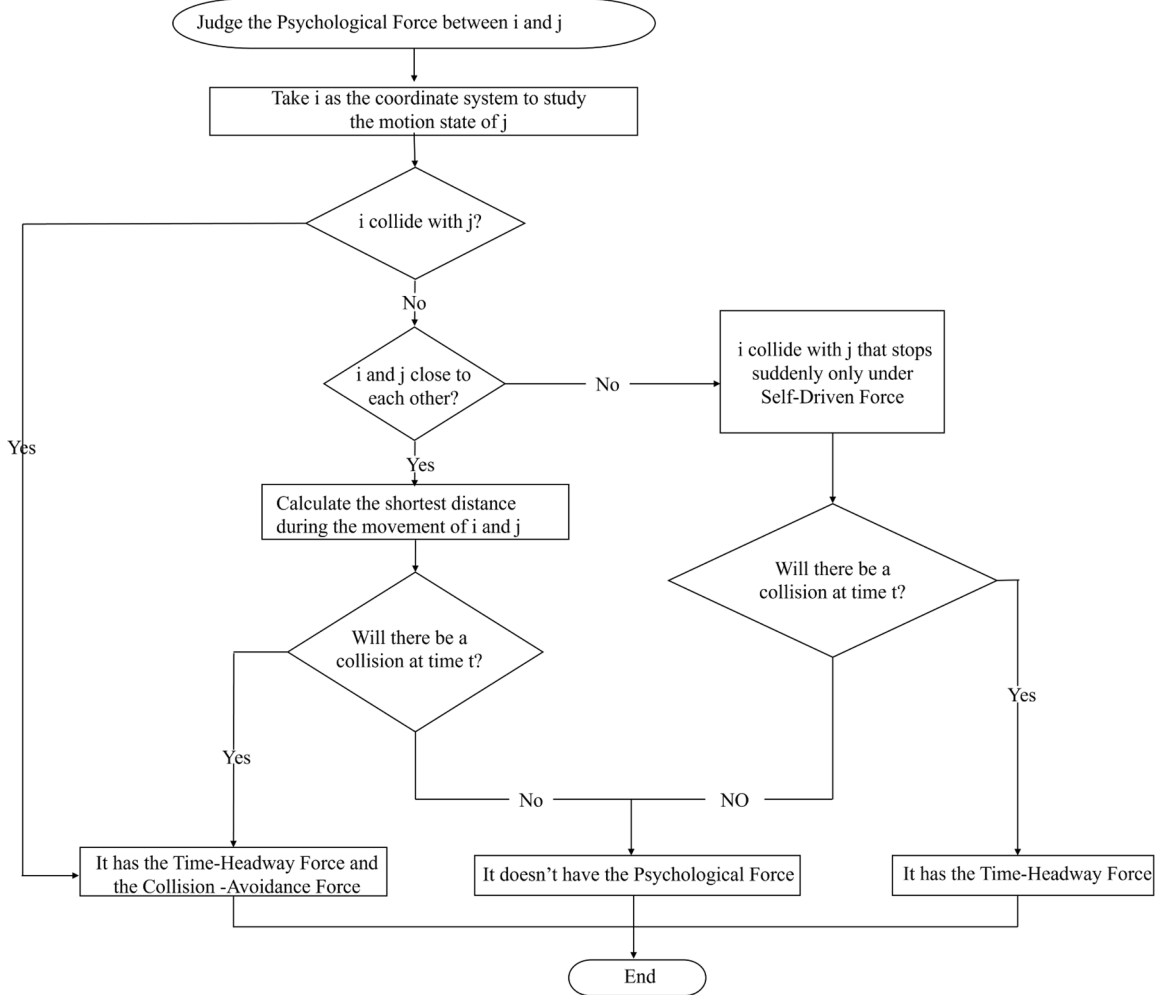


Fig. 6. Schematic diagram of time-headway force generation.



**Fig. 7.** Flowchart of psychological analysis in MSF.

#### 4.1. Simulation 1: validation based on the experiments

To validate MSF, we set up the same scenario as the one in the Jülich evacuation database<sup>1</sup> for simulation. In Jülich evacuation database, the experimental set-up consisted of a rudimentary room built in the schools' assembly hall. [64] This room was a square area of  $5 \times 5$  m bounded by small buckets on three sides (see Fig. 8). There was a door on one side of the experimental area and the widths of the door is 1.4 m.

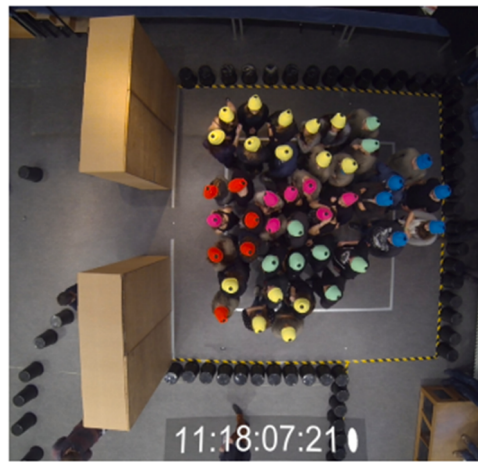
The parameters and building layout of the simulation were set up based on the experiments. The size of the standard room to simulate evacuation scene is  $5 \text{ m} \times 5 \text{ m}$ , and the number of pedestrians is 42. We conducted 8 sets of simulation experiments under the same conditions to compare with the Jülich experiment results. Each pedestrian is regarded as a circle with a radius of 0.21 m in the simulation, and the width of the exit is 1.4 m. The snapshots of the simulation process were shown in Fig. 9.

Fig. 10(a) displays the findings of the experiments' evacuation time and cumulative number of evacuated pedestrians, and Fig. 10 displays the simulation's results Fig. (b) According to the results in Fig. 10, we can see that the simulation results of MSF are basically the same as the experimental results of Jülich. With the equal numbers of evacuees, the overall evacuation time differs by less than one second. After comparison, it is found that the simulation results are acceptable and have a good accuracy.

#### 4.2. Simulation 2: the interaction between pedestrians and the wall

Under the support of the MSF, we are going to analyze the Table-Tennis phenomenon mentioned above that exists in SF. It happens

<sup>1</sup> <https://ped.fz-juelich.de/da/doku.php>



**Fig. 8.** The image of Jülich evacuation experiment.

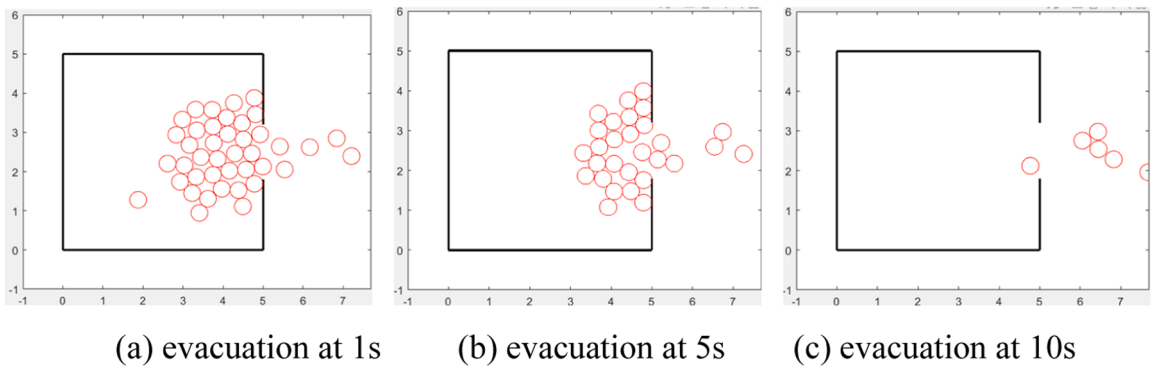


**Fig. 9.** Snapshots of the simulation.

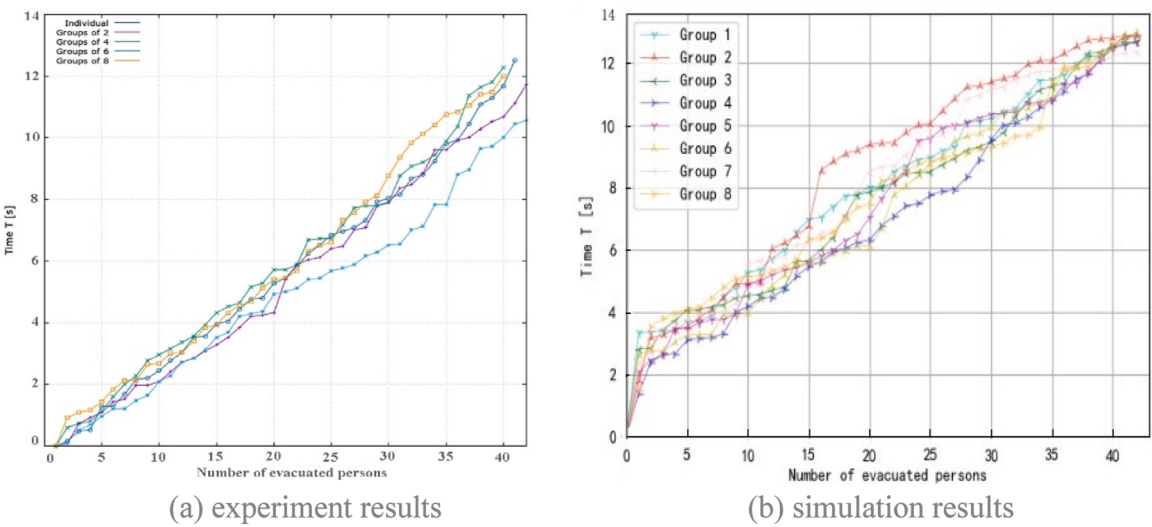
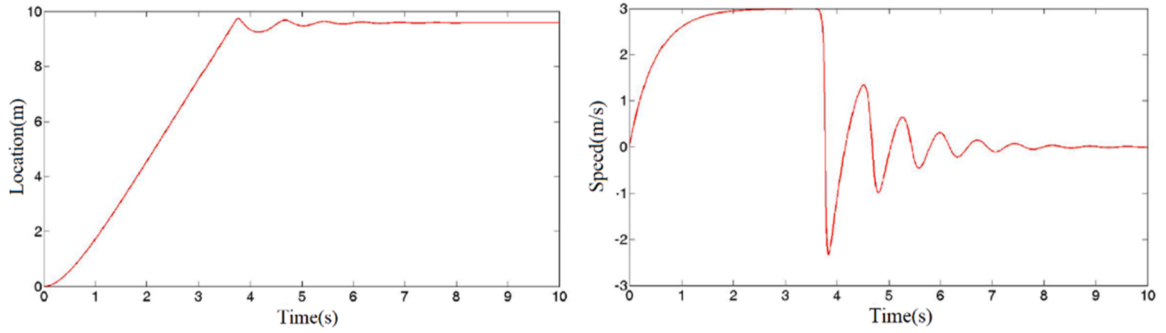
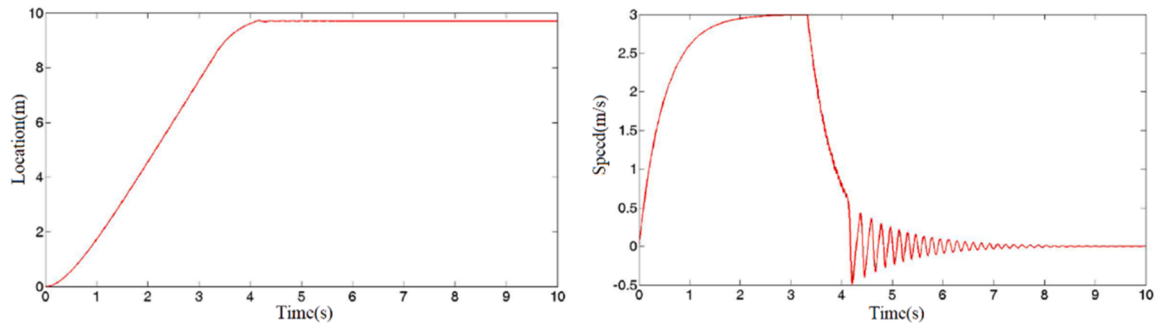


**Fig. 10.** The evacuation time results of the experiment and our simulation.



(a) Displacement simulation results      (b) Velocity simulation results

Fig. 11. schematic diagram of SF oscillation.



(a) Displacement simulation results      (b) Velocity simulation results

Fig. 12. schematic diagram of GSF oscillation.

when pedestrians collide with the wall. Fig. 11 shows the curve of simulator's displacement and change of speed in the process of moving toward the wall from 10 m away, at the expected speed of 3 m/s under SF. Fig. 12 shows the weakening of displacement and velocity oscillations after the improvement of GSF.

In the results of SF, the oscillation of velocity is very evident. It means that in the simulation, personnel will repeatedly carry out the movements of collision-rebound-deceleration-collision at the wall, which is inconsistent with the actual situation. After modifying GSF, the oscillation of velocity has been greatly alleviated, but the nature of oscillation has not changed. Therefore, we will analyze the stress condition in this movement process. When a pedestrian is moving towards the wall, we can remember the direction towards the wall as positive, so that the equation of its motion state is:

$$F_D - F_S - F_P = ma \quad (27)$$

The specific analysis of movement process is shown as follows:

**Stage 1.** there's no collision with the wall  $F_P = 0$ , have nor arrived at the place near the wall  $F_S=0$ . There is only a self-driven force at this moment. The pedestrian accelerates to the desired speed  $v_0$  within time  $\tau$  and maintains a uniform speed. The moving speed is facing the wall.

**Stage 2.** there is no collision with the wall  $F_P = 0$ , when it arrives near the wall, collision-avoidance force and time-headway force are generated. The self-driven force is still playing a role. Pedestrian obtains the acceleration  $\alpha$ . We assumed that when stage 2 happens, the initial velocity of pedestrian is  $v_1$ :

$$ma = m \frac{v_0 - v_t}{\tau} - \left( m \frac{v_0}{\tau} - m \frac{v_t}{\tau} + m \frac{v_t}{\tau} \right) \quad (28)$$

$$a = -\frac{v_t}{\tau} \quad (29)$$

The movement speed of pedestrian change as follows:

$$\frac{dv_t}{dt} = -\frac{v_t}{\tau} \quad (30)$$

$$v_t = v_1 e^{-\frac{t}{\tau}} \quad (31)$$

We can see that the pedestrian is constantly decelerating at this time. With the decrease of speed, the deceleration is also getting slower, until it collides with the wall. The moving speed direction is always towards the wall.

**Stage 3.** collide with the wall,  $F_p > 0$  and the direction is away from the wall. The pedestrian's current traveling speed is still more than 0. The extrusion amount continues to increase. The psychological force exists, and the acceleration of pedestrians is calculated by Eq. (32).

$$a = -\frac{k}{m}\epsilon - \frac{v_t}{\tau} \quad (32)$$

At this time,  $\alpha < 0$  is constantly established. The pedestrian's moving speed will decrease to 0 rapidly, and then reverse towards the direction away from the wall.

**Stage 4.** continue colliding with the wall,  $F_p > 0$  and the direction is away from the wall, the moving speed of pedestrian is less than 0, and the extrusion amount decreases continuously. There is no colliding object in the moving direction of the pedestrian, so the psychological force disappears, and the self-driven force still exists. The acceleration of the pedestrian is calculated by Eq. (33).

$$a = -\frac{k}{m}\epsilon + \frac{v_0 - v_t}{\tau} \quad (33)$$

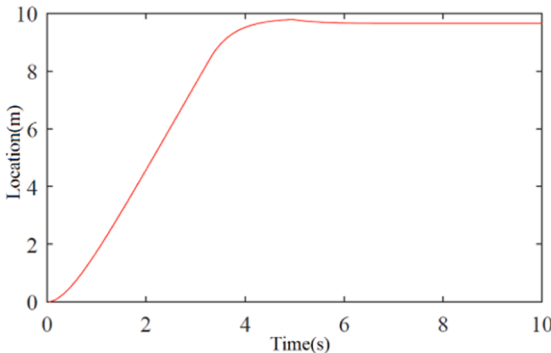
When the extrusion amount is decreased to a certain degree, that is, when  $\epsilon < m(v_0 - -v_t)/k\tau$ , the acceleration is reversed again, and the pedestrian starts to accelerate towards the wall again until the moving speed is reversed to the direction towards the wall.

**Stage 5.** At this time, the direction of pedestrian's moving speed faces the wall. The self-driven force and the psychological force exist. The elasticity of the wall may exist, and the motion state is also determined by Eq. (34). After that, the pedestrian's motion state will cycle repeatedly between stage 3 and stage 4. The oscillation phenomenon illustrated in Fig. 12 appears.

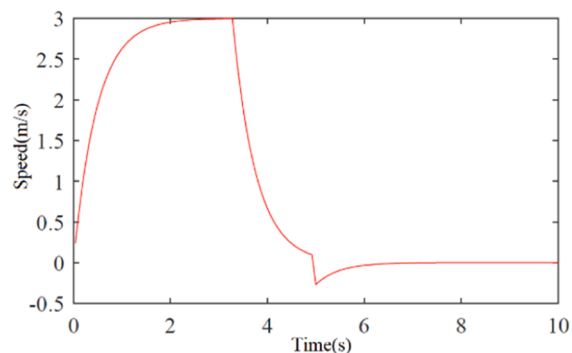
An analysis of the aforementioned movement process reveals that, at this point, collision prediction after  $\tau$  is solely based on the individual's current movement speed, followed by an assessment of whether psychological force has been triggered. Notably, the psychological force abruptly vanishes when the individual encounters a wall. The pedestrian obtains the acceleration towards the wall under the action of self-driven force. When the pedestrian's moving speed turns back towards the wall again, the psychological force will be regenerated and repeat the previous movement process. It eventually leads to pedestrians' repeated oscillation phenomenon at the wall.

However, in the MSF of this paper, the judgment of psychological force considers not only the moving speed of personnel, but also the acceleration of personnel. We simulate the above moving process in a similar way, and the results are shown in Fig. 13. The oscillation phenomenon completely disappears, which is shown in the process of pedestrians approaching the wall. They would first decelerate under the action of psychological force. After they collide with the wall, the psychological force still exists and balances with the self-driven force. The acceleration generated by the combined force of the two is  $-v_t/\tau$ , which slowly rebounds to the compression amount 0 and remains stationary. This process is more in line with the actual situation and the process curve is smoother.

Further, we found that when a pedestrian continues to move towards the wall until the moment when psychological force generates, the distance between the pedestrian and the wall is  $v_1\tau$ . We can calculate the displacement state of the pedestrian:



(a) the simulation results of displacement



(b) simulation results of velocity

Fig. 13. schematic diagram of repairing MSF oscillation phenomenon.

$$x_t = \int_0^t v_1 e^{-\frac{t}{\tau}} dt \quad (35)$$

$$\lim_{t \rightarrow \infty} x_t = v_1 \tau \quad (36)$$

Moreover, we can find that under the setting of psychological force in the MSF in this paper,  $x_t$ 's monotonically convergent. That is, whenever  $\forall t > 0$ , there will be  $x_t < v_1 \tau$ . It means that in the actual calculation process, the limit displacement of the pedestrian in his process of moving towards the wall is  $v_1 \tau$ . Theoretically speaking, the pedestrian will never collide with the wall. The speed of the pedestrian will be reduced to 0 just when he reaches the wall in the limit state. The reason that collision and rebound phenomenon occur in the simulation, is that we must use discrete time steps to calculate in the model simulation state. In the last time step, the displacement of pedestrians will exceed the limit value of theoretical calculation, resulting in the collision in the simulation. The above analysis shows that the smaller the time step is set in the simulation process, the smaller the compression amount of collision with the wall will be. Fig. 14 respectively shows the speed change curve when the calculation step is 0.08 s, 0.04 s and 0.02 s, which is consistent with the above conclusion. At the same time, it is noted that even if the collision between pedestrians and walls occurs due to the discrete-time characteristics of computer simulation, the oscillation phenomenon in SF and GSF will not occur since we have modified the conditions of generating the psychological force in the improved social force model.

#### 4.3. Simulation 3: the crowd evacuation in rooms

The size of the standard room to simulate evacuation scene is  $9 m \times 9 m$ . Take the state of the 10th and 15th seconds, and the number of pedestrians is 25, 50, 100, 150 and 200 respectively. It can be seen from Figs. 15 and 16 that when time is 10 s, a typical state of Arched Congestion appears as the number of evacuees increases. [65] The arched congestion phenomenon is the most significant when the evacuee number is 100.

As shown in the Fig. 17, the red circle represents pedestrians, with a total number of 150. The pedestrian is regarded as a circle with a radius of 0.21 m in the model. They evacuate through the exit on the right side, whose width is 0.8 m.

In the condition of same exit width and same competitiveness, we can analyze the impact of different initial evacuee numbers on the evacuation results: When the overall competitiveness is 0, under the condition of the same exit width, there will be more evacuation flow when the initial number of pedestrians is larger in this simulation. It is due to the reason that in the simulation, a bigger initial number of pedestrians means a higher density. According to the research done in many documents, within a certain density range, the increase of crowd density will increase the flow of personnel. Therefore, in the situation of personnel passing through the outlet orderly, its flow will be larger.

Under the same competitiveness and different initial evacuee numbers, the impact of exit width on evacuation results: when the initial evacuee number is 25 and the exit width is 0.8 m, 1.4 m and 2.0 m, the flow increases with the increase of exit width, which is the same as the real situation.

In summary, the simulation findings show that, for a given exit width, the evacuation flow increases with the initial number of evacuees. The possible reason for this phenomenon is that crowd density affects evacuation in two different ways. On the one hand, when the crowd density is high, the motivation of pedestrians to keep a certain distance is weakened, which increases the utilization of space and improves the evacuation speed; On the other hand, the increase of crowd density makes pedestrians more inclined to generate pushing and shoving behaviors. When the evacuation environment is not ideal such as the instance where the exit is narrow, it is very likely to occur congestion, which will further decrease the evacuation efficiency. When the competitiveness is the same, the larger the exit width is, the greater the evacuation flow will be.

#### 5. Conclusion

Based findings from prior studies, the setting mode of the psychological force in the social force model has been improved in this work. The GSF model sets the time-headway force too large, resulting in direct cessation of movement when facing stationary obstacles, and reverse movement when facing impending collisions with obstacles. To address this issue, this study further improves the time-headway force and collision-avoidance force. In terms of psychological force values, only the psychological force generated by pedestrians in front of the obstacles is considered, while pedestrians behind are no longer consideration, which is a key difference between MSF and GSF. In terms of psychological force determination, GSF only considers the current velocity without taking acceleration into account. However, MSF considers not only the current velocity but also the effect of acceleration. In the MSF, the speed changes more smoothly in different scenes, and the Table-Tennis phenomenon that exists in Helbing's social force model, which means evacuees' speed oscillates near fixed obstacles, is eliminated. When simulating the evacuation process of pedestrians in the room, we found that this model well reproduces the Arch Congestion phenomenon in the evacuation process, which proves that the model is effective and characteristic in its simulation of the horizontal evacuation process in the building.

In future researches, we will expand the scope of experiment samples of evacuation in buildings. We will deepen the evacuation behavior characteristics and decision-making preferences of different characteristic groups. In the evacuation experiments, we will gather more information from samples representing a variety of genders, ages, occupations, and educational backgrounds; we will design a number of evacuation-guiding techniques and offer combined schemes, optimizing the overall intervention plan for evacuation in the building; we will conduct real experiments in various complex scenarios, gather more experiment data and analyze all

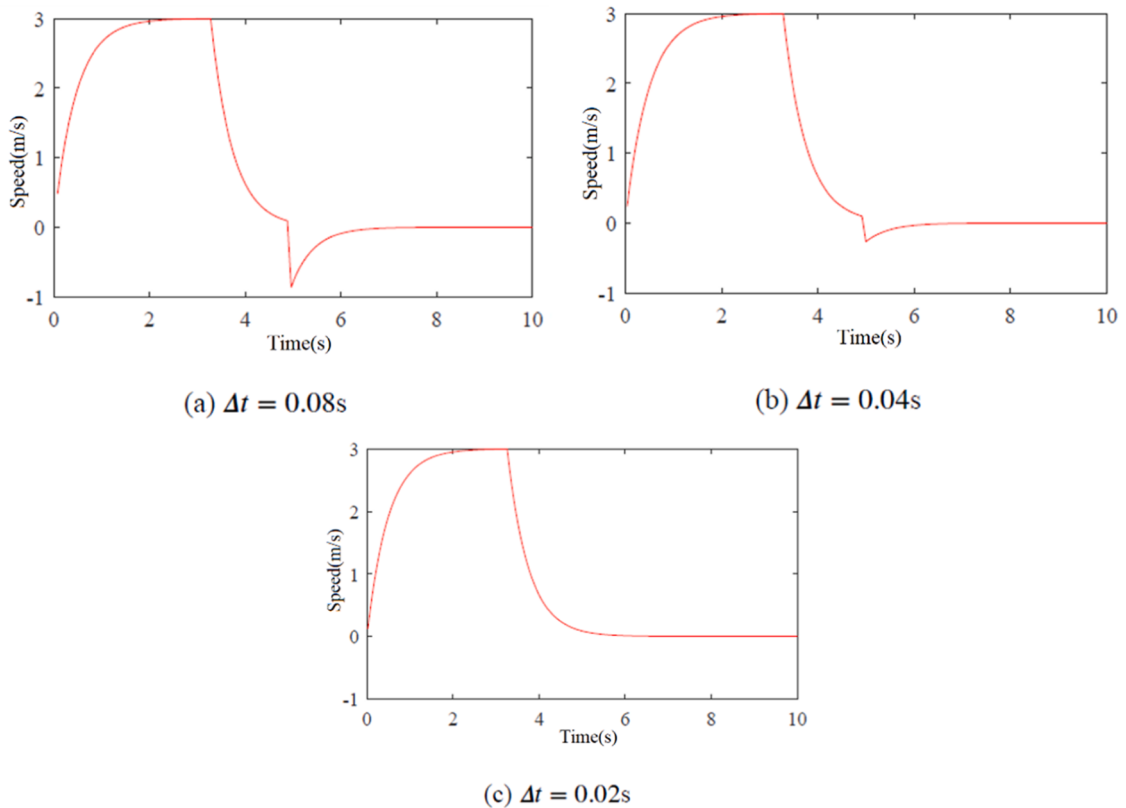


**Fig. 14.** the velocity variation curve under the conditions of different calculation steps.

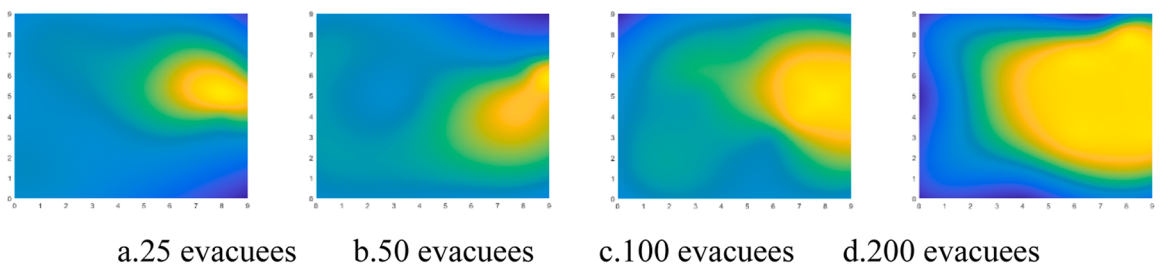


**Fig. 15.** The heat diagram for evacuation at 10 s.

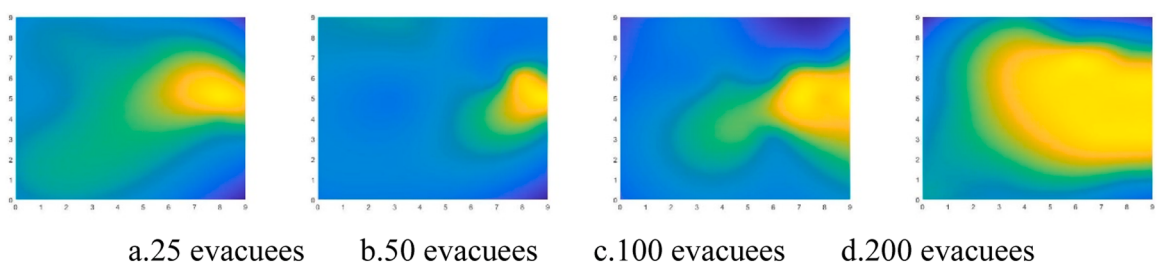
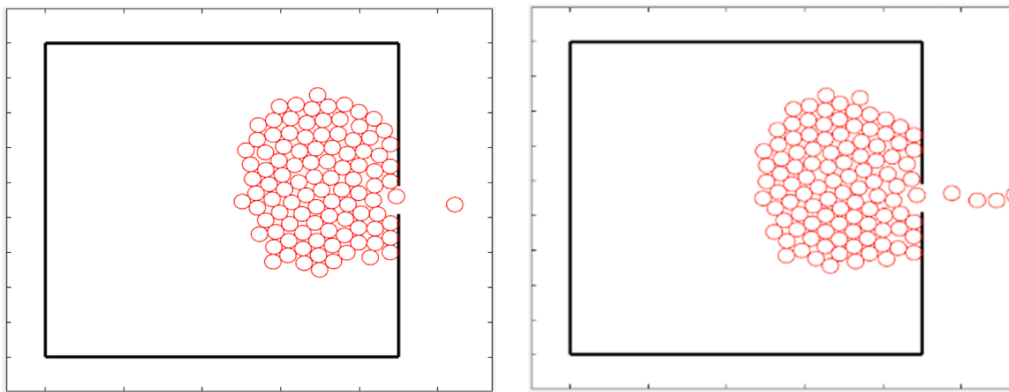
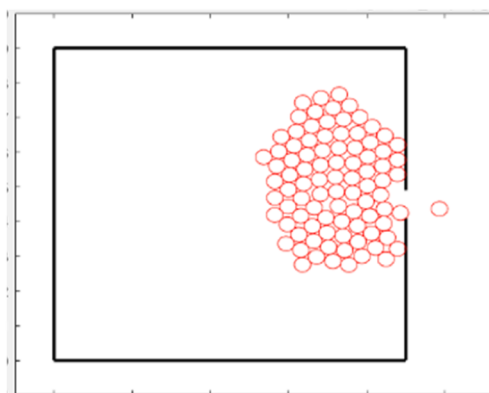


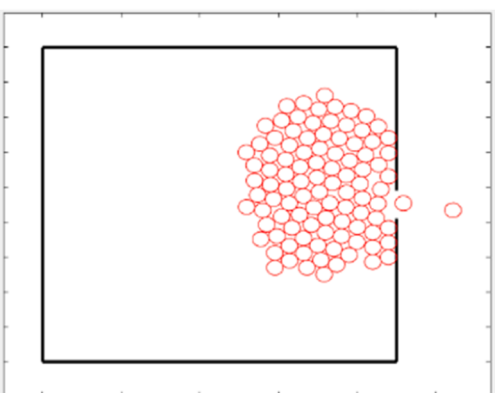
**Fig. 16.** The heat diagram for evacuation at 15 s.



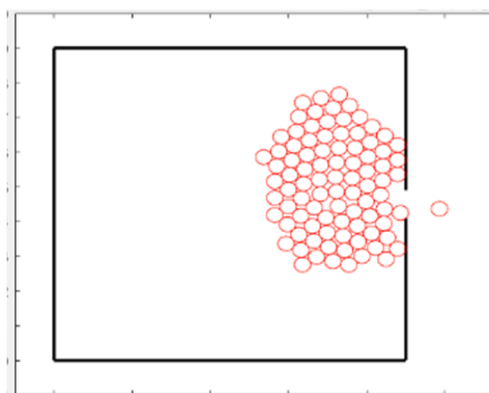
a. the condition of 150 evacuees at 10s



b. the condition of 150 evacuees at 12s



c. the condition of 150 evacuees at 14s



d. the condition of 150 evacuees at 16s

**Fig. 17.** Arched Congestion.

kinds of influencing factors through machine learning[66] to improve the accuracy of models as well as experimental findings.

#### Data availability

No data was used for the research described in the article.

#### Acknowledgement

This work is supported by the National Natural Science Foundation of China (72274208), Basic Research Foundation of People's Public Security University of China (2022JKF02010) and the Public Security First-class Discipline Cultivation and Public Security Behavioral Science Lab Project (No.2023ZB02).

#### Appendix

This appendix provides the address for finding the simulation model source code network.

Address:<https://github.com/erhao12345678/social-force-model>

#### References

- [1] M. Jusup, P. Holme, K. Kanazawa, M. Takayasu, I. Romić, Z. Wang, M. Perc, Social physics, *Phys. Rep.* 948 (2022) 1–148.

- [2] M. Perc, The social physics collective, *Sci Rep* 9 (1) (2019) 16549.
- [3] L.F. Henderson, On the fluid mechanics of human crowd motion, *Transp. Res.* 8 (6) (1974) 509–515.
- [4] Helbing, D. (1998). A fluid dynamic model for the movement of pedestrians. *arXiv preprint cond-mat/9805213*.
- [5] L.F. Henderson, The statistics of crowd fluids, *Nature* 229 (5284) (1971) 381–383.
- [6] C.W. Johnson, Lessons from the evacuation of the world trade centre, 9/11 2001 for the development of computer-based simulations, *Cognit. Technol. Work* 7 (2005) 214–240.
- [7] D. Helbing, P. Molnar, Social force model for pedestrian dynamics, *Phys Rev E* 51 (5) (1995) 4282.
- [8] C. Burstedde, K. Klauck, A. Schadschneider, J. Zittartz, Simulation of pedestrian dynamics using a two-dimensional cellular automaton, *Phys. A Stat. Mech. Appl.* 295 (3–4) (2001) 507–525.
- [9] A. Kirchner, A. Schadschneider, Simulation of evacuation processes using a bionics-inspired cellular automaton model for pedestrian dynamics, *Phys. A Stat. Mech. Appl.* 312 (1–2) (2002) 260–276.
- [10] C.G. Langton, Self-reproduction in cellular automata, *Phys. D Nonlin. Phenom.* 10 (1984) 135–144.
- [11] R. Lovreglio, A. Fonzone, L. Dell’Olio, D. Borri, A study of herding behaviour in exit choice during emergencies based on random utility theory, *Saf. Sci.* 82 (2016) 421–431.
- [12] P. Lin, D.L. Gao, G.Y. Wang, F.Y. Wu, J. Ma, Y.L. Si, T. Ran, The impact of an obstacle on competitive evacuation through a bottleneck, *Fire Technol* 55 (2019) 1967–1981.
- [13] A.S. Mohammed, A. Pavic, Simulation of people’s movements on floors using social force model, in: *Proceedings of the Dynamics of Civil Structures, Volume 2: Proceedings of the 36th IMAC, A Conference and Exposition on Structural Dynamics 2018*, Springer International Publishing, 2019, pp. 39–46.
- [14] J. Wan, J. Sui, H. Yu, Research on evacuation in the subway station in China based on the Combined Social Force Model, *Phys. A Stat. Mech. Appl.* 394 (2014) 33–46.
- [15] Q. Liu, A social force model for the crowd evacuation in a terrorist attack, *Phys. A Stat. Mech. Appl.* 502 (2018) 315–330.
- [16] R. Zhou, Y. Cui, Y. Wang, J. Jiang, A modified social force model with different categories of pedestrians for subway station evacuation, *Tunnel. Undergr. Space Technol.* 110 (2021), 103837.
- [17] H. Zhang, H. Liu, X. Qin, B. Liu, Modified two-layer social force model for emergency earthquake evacuation, *Phys. A Stat. Mech. Appl.* 492 (2018) 1107–1119.
- [18] J. Wan, J. Sui, Emergency evacuation in subway station based on combined social force model, in: *Proceedings of the IEEE International Conference on Electronics Information and Emergency Communication*, Beijing, China, 2014, pp. 242–245.
- [19] P.A. Langston, R. Masling, B.N. Asmar, Crowd dynamics discrete element multi-circle model, *Saf. Sci.* 44 (5) (2006) 395–417.
- [20] D.R. Parisi, M. Gilman, H. Moldovan, A modification of the social force model can reproduce experimental data of pedestrian flows in normal conditions, *Phys. A Stat. Mech. Appl.* 388 (17) (2009) 3600–3608.
- [21] O. Hosseini, M. Maghrebi, Risk of fire emergency evacuation in complex construction sites: integration of 4D-BIM, social force modeling, and fire quantitative risk assessment, *Adv. Eng. Inform.* 50 (2021), 101378.
- [22] B. Steffen, A modification of the social force model by foresight, *Pedestrian and Evacuation Dynamics 2008*, Springer Berlin Heidelberg, 2010, pp. 677–682.
- [23] J. Zhang, H. Liu, Y. Li, X. Qin, S. Wang, Video-driven group behavior simulation based on social comparison theory, *Phys. A Stat. Mech. Appl.* 512 (2018) 620–634.
- [24] S. Weiguo, Y. Yanfei, C. Tao, Influence of exit condition on evacuation and analysis, *Fire Sci.* 12 (2) (2003) 100–104.
- [25] J. Wang, W. Zhu, M. Yin, S. Zhong, Emergency Evacuation From a Teaching Building Based on The Social Force Model, in: *Proceedings of the IEEE 2021 IEEE 11th International Conference on Electronics Information and Emergency Communication (ICEIEC)*, IEEE, 2021, pp. 1–7.
- [26] H. Benseghir, A.B. Ibrahim, M.N.I. Siddique, M.N. Kabir, Y.M. Alginah, Modelling emergency evacuation from an industrial building under spreading fire using a social force model with fire dynamics, *Mater. Today Proc.* 41 (2021) 38–42.
- [27] Z. Kang, L. Zhang, K. Li, An improved social force model for pedestrian dynamics in shipwrecks, *Appl. Math. Comput.* 348 (2019) 355–362.
- [28] Y. Han, H. Liu, Modified social force model based on information transmission toward crowd evacuation simulation, *Phys. A Stat. Mech. Appl.* 469 (2017) 499–509.
- [29] F. Zanlungo, T. Ikeda, T. Kanda, Social force model with explicit collision prediction, *Europhys. Lett.* 93 (6) (2011) 68005.
- [30] L. Cambium, E. Barros, Fpga-based pedestrian detection for collision prediction system, *Sensors* 22 (12) (2022) 4421.
- [31] N. Rinke, C. Schiermeyer, F. Pascucci, V. Berkahn, B. Friedrich, A multi-layer social force approach to model interactions in shared spaces using collision prediction, *Transport. Res. Proc.* 25 (2017) 1249–1267.
- [32] K. El-Basyouny, T. Sayed, Collision prediction models using multivariate Poisson-lognormal regression, *Accid. Anal. Prevent.* 41 (4) (2009) 820–828.
- [33] V.J. Blue, J.L. Adler, Cellular automata microsimulation of bidirectional pedestrian flows, *Transp. Res. Rec.* 1678 (1) (1999) 135–141.
- [34] H. Klüpfel, T. Meyer-König, J. Wahle, M. Schreckenberg, Microscopic simulation of evacuation processes on passenger ships, in: *Proceedings of the Theory and Practical Issues on Cellular Automata: Proceedings of the Fourth International Conference on Cellular Automata for Research and Industry*, Karlsruhe, 4–6 October 2000, Springer London, London, 2001, pp. 63–71.
- [35] W.G. Weng, T. Chen, H.Y. Yuan, W.C. Fan, Cellular automaton simulation of pedestrian counter flow with different walk velocities, *Phys. Rev. E* 74 (3) (2006), 036102.
- [36] C.Y. Li, R.Y. Yang, G.M. Xu, Impacts of group behavior on boarding process at the platform of high speed railway station, *Phys. A Stat. Mech. Appl.* 535 (2019), 122247.
- [37] M. Shi, E.W.M. Lee, Y. Ma, A novel grid-based mesoscopic model for evacuation dynamics, *Phys. A Stat. Mech. Appl.* 497 (2018) 198–210.
- [38] M. Shi, E.W.M. Lee, Y. Ma, A dynamic impatience-determined cellular automata model for evacuation dynamics, *Simul. Model. Pract. Theor.* 94 (2019) 367–378.
- [39] X. Li, T. Chen, L. Pan, S. Shen, H. Yuan, Lattice gas simulation and experiment study of evacuation dynamics, *Phys. A Stat. Mech. Appl.* 387 (22) (2008) 5457–5465.
- [40] F. Huo, W. Song, W. Lv, K.M. Liew, Analyzing pedestrian merging flow on a floor–stair interface using an extended lattice gas model, *Simulation* 90 (5) (2014) 501–510.
- [41] B. Maury, J. Venel, A mathematical framework for a crowd motion model, *Compt. Rendus Math.* 346 (23–24) (2008) 1245–1250.
- [42] J. Van den Berg, M. Lin, D. Manocha, Reciprocal velocity obstacles for real-time multi-agent navigation, in: *Proceedings of the 2008 IEEE international conference on robotics and automation*, Ieee, 2008, pp. 1928–1935.
- [43] G. Rockenbach, C. Boeira, D. Schaffer, A. Antonitsch, S.R. Musse, Simulating crowd evacuation: from comfort to panic situations, in: *Proceedings of the 18th International Conference on Intelligent Virtual Agents*, 2018, pp. 295–300.
- [44] F. Weifeng, Y. Lizhong, F. Weicheng, Simulation of bi-direction pedestrian movement using a cellular automata model, *Phys. A Stat. Mech. Appl.* 321 (3–4) (2003) 633–640.
- [45] H. Selamat, N. Khamis, N. Mohd Ghani, Crowd modeling and simulation for safer building design, *Int. J. Electr. Comput. Eng. Syst.* 11 (2) (2020) 77–88.
- [46] W.J. Yu, R. Chen, L.Y. Dong, S.Q. Dai, Centrifugal force model for pedestrian dynamics, *Phys. Rev. E* 72 (2) (2005), 026112.
- [47] D.M. Shi, B.H. Wang, Evacuation of pedestrians from a single room by using snowdrift game theories, *Phys. Rev. E* 87 (2) (2013), 022802.
- [48] M. Chraibi, A. Tordeux, A. Schadschneider, A. Seyfried, Modelling of pedestrian and evacuation dynamics, *Encycloped. Complex. Syst.* (2018) 1–22.
- [49] A. Seyfried, B. Steffen, T. Lippert, Basics of modelling the pedestrian flow, *Phys. A Stat. Mech. Appl.* 368 (1) (2006) 232–238.
- [50] Tao Chen, Z.Y. Ying, Sf Shen, Hongyong Yuan, W.C. Fan, Social force model evacuation simulation and analysis under relative velocity impact, *Prog. Nat. Sci.* 16 (2006) 1606–1612.
- [51] Y. Gao, P.B. Luh, H. Zhang, T. Chen, A modified social force model considering relative velocity of pedestrians, in: *Proceedings of the 2013 IEEE International Conference on Automation Science and Engineering (CASE)*, IEEE, 2013, pp. 747–751.

- [52] T.I. Lakoba, D.J. Kaup, N.M. Finkelstein, Modifications of the Helbing-Molnar-Farkas-Vicsek social force model for pedestrian evolution, *Simulation* 81 (5) (2005) 339–352.
- [53] M. Apel, Simulation of pedestrian flows based on the social force model using the verlet link cell algorithm, *Poznan Univ. Technol.* 79 (2004).
- [54] Q. Ji, H. He, F. Wang, Social force model for crowd simulation using density field), *Peer. J. Comput. Sci.* 42 (6) (2015) 12–17.
- [55] S.S. Li, D.L. Qian, J.Z. Wang, Improved social force model considering pedestrian deceleration to avoid collision, *J. Jilin Univ. (Eng. Technol. Ed.)* 42 (3) (2012) 623–628.
- [56] M.J. Quinn, R.A. Metoyer, K. Hunter-Zaworski, Parallel implementation of the social forces model, in: Proceedings of the Second International Conference in Pedestrian and Evacuation Dynamics 63, 2003, p. 74.
- [57] D.J. Kaup, T.L. Clarke, R. Oleson, L. Malone, F.G. Jentsch, Introducing age-based parameters into simulations of crowd dynamics, in: Proceedings of the 2008 Winter Simulation Conference, IEEE, 2008, pp. 895–902.
- [58] D. Zhang, G. Huang, C. Ji, H. Liu, Y. Tang, Pedestrian evacuation modeling and simulation in multi-exit scenarios, *Phys. A Stat. Mech. Appl.* 582 (2021), 126272.
- [59] Q. Liu, L. Lu, Y. Zhang, M. Hu, Modeling the dynamics of pedestrian evacuation in a complex environment, *Phys. A Stat. Mech. Appl.* 585 (2022), 126426.
- [60] L. Hou, J.G. Liu, X. Pan, B.H. Wang, A social force evacuation model with the leadership effect, *Phys. A Stat. Mech. Appl.* 400 (2014) 93–99.
- [61] Q. Li, Y. Liu, Z. Kang, K. Li, L. Chen, Improved social force model considering conflict avoidance, *Chaos An Interdiscipl. J. Nonl. Sci.* 30 (1) (2020).
- [62] X. Chen, M. Treiber, V. Kanagaraj, H. Li, Social force models for pedestrian traffic—state of the art, *Transp. Rev.* 38 (5) (2018) 625–653.
- [63] Y. Gao, T. Chen, P.B. Luh, H. Zhang, Modified social force model based on predictive collision avoidance considering degree of competitiveness, *Fire Technol* 53 (1) (2017) 331–351.
- [64] C. Von Krüchten, A. Schadschneider, Empirical study on social groups in pedestrian evacuation dynamics, *Phys. A Stat. Mech. Appl.* 475 (2017) 129–141.
- [65] D. Helbing, I.J. Farkas, P. Molnar, T. Vicsek, Simulation of pedestrian crowds in normal and evacuation situations, *Pedest. Evacuat. Dyn.* 21 (2) (2002) 21–58.
- [66] L. Yang, N. Ding, Evacuation behavior under violent attacks in classrooms based on experiments and interpretable machine learning method, *Saf Sci* 166 (2023), 106243.